A Calorimetric Investigation of a Series of Mixed-Chain Polyunsaturated Phosphatidylcholines: Effect of *sn*-2 Chain Length and Degree of Unsaturation

Charles D. Niebylski and Norman Salem, Jr.

Section of Fluorescence Studies, Laboratory of Membrane Biochemistry and Biophysics, DICBR, NIAAA, National Institutes of Health, Rockville, Maryland 20852 USA

ABSTRACT Although mammalian tissues contain high levels of polyunsaturated fatty acids, our knowledge of the effects of the degree of unsaturation and double-bond location upon bilayer organization is limited. Therefore, a series of mixed-chain unsaturated phosphatidylcholines (PC) comprised of 18:0 at the *sn*-1 position and various unsaturates at the *sn*-2 position (18:1n9, 18:2n6, 18:3n6, 18:3n3, 20:2n6, 20:3n6, 20:4n6, 20:5n3, 22:4n6, 22:5n3, 22:5n6, or 22:6n3) was studied with differential scanning calorimetry, and their gel to liquid-crystalline phase transitions yielded measurements of T_m, T_{onset}, ΔH, and ΔS. Minimal ΔH values were obtained for the diene species, 1.7 and 2.9 kcal/mole for 18:2n6 and 20:2n6, respectively. These results are consistent with the dienes having an acyl chain conformation that results in perturbed chain packing. Increasing the degree of unsaturation to three or more double bonds resulted in higher ΔH values, 3.7, 4.3, and 4.6 kcal/mole for 18:3n6, 20:3n6, and 20:4n6, respectively, consistent with the occurrence of a gel-state chain conformation(s), which is more tightly packed than the dienes. The 18:0,22:6n3-PC species yielded the highest ΔH (6.1 kcal/mole) and ΔS (22.7 cal/mol°) of all the polyunsaturates studied. The distinctive packing properties of phospholipid bilayers containing 22:6n3 may underlie its essential role in the nervous system.

INTRODUCTION

Polyunsaturated fatty acids are commonly found in the phospholipids comprising biological membranes with the most highly unsaturated species concentrated in cells involved in information processing such as the neuron, rod cells, and sperm (Salem et al., 1986, 1989). Docosahexaenoic acid (22:6n3) serves an essential role in the maintenance of optimal synaptic and retinal function, and when 22:5n6 is substituted for this fatty acid after dietary modification, functional impairments are observed (Salem et al., 1986, 1989; Salem and Ward, 1993). It is clear that there is little information concerning differences in biophysical properties or functions between these two species. However, recent work has indicated that a cyclooxygenase or lipoxygenase metabolite of 22:6n3 is not responsible for this function (Kim et al., 1991), and it has been suggested that a membrane property of the 22:6n3-phospholipid is critical (Salem and Niebylski, 1995). Thus, it is of great importance that the biochemical and biophysical properties of various unsaturated phospholipids be described and compared.

Effects of polyunsaturated phospholipid composition upon membrane protein function have been documented by many investigators (Mitchell et al., 1992; for a review, see Stubbs and Smith, 1987). Many studies of reconstituted polyunsaturated phospholipid bilayer models have focused mainly on lipids containing two polyenoic acyl chains (at the *sn*-1 and *sn*-2 positions); yet these are usually found only in low percentages or in highly specialized membranes (Dratz and Deese, 1986). In most studies of mixed-chain phospholipids, palmitic acid (16:0) has been employed at the *sn*-1 position (Straume and Litman, 1987; Stubbs, 1993; Baenziger et al., 1992), although stearate (18:0) as the *sn*-1 saturate has been used in a few studies (Coolbear et al., 1983; Ehringer et al., 1991). In this study, we have chosen stearate (18:0) as our *sn*-1 position saturate because it is the predominate fatty acid with which long chain polyunsaturates are paired in neural membranes (Salem, 1989). For example, 18:0 comprises essentially all of the fatty acid at *sn*-1 in brain phosphatidylserine (PS) (Salem et al., 1976).

Phospholipids containing 22:6n3 have been shown to provide maximal rhodopsin meta-II concentration (Mitchell et al., 1992; Wiedmann et al., 1988) and protein kinase C activation (Slater et al., 1994) in reconstituted phospholipid bilayer model systems. The physical characteristics of 22:6n3-containing bilayers include minimal DPH fluorescence anisotropy order parameters, indicating maximal perturbation of the acyl chain domain (Straume and Litman, 1987; Salem and Niebylski 1993; Niebylski and Salem, 1994; Stubbs, 1993), and microclustering of 16:0,22:6n3-phosphatidylcholine molecules, which is suggested by

Received for publication 27 June 1994 and in final form 20 September 1994.

Address reprint requests to Norman Salem, Jr., LMBB/NIAAA/National Institutes of Health, 12501 Washington Ave., Rockville, MD 20852. Fax: 301-594-0035; E-mail: nzz@cu.nih.gov.

Abbreviations used: BHT, butylated hydroxytoluene; DSC, differential scanning calorimetry; HPLC, high performance liquid chromatography; NMR, nuclear magnetic resonance; PUFA, polyunsaturated fatty acid; PC, phosphatidylcholine; PE, phosphatidylethanolamine; PS, phosphatidylserine; T_m, peak melting temperature; ΔH, transition enthalpy; ΔS, transition entropy. Double-bond location for each of the fatty acids is designated as follows: 18:1n9$^{\Delta 9}$, 18:2n6$^{\Delta 9,12}$, 18:3n6$^{\Delta 6,9,12}$, 18:3n3$^{\Delta 9,12,15}$, 20:2n6$^{\Delta 11,14}$, 20:3n6$^{\Delta 8,11,14}$, 20:4n6$^{\Delta 5,8,11,14}$, 20:5n3$^{\Delta 5,8,11,14,17}$, 22:4n6$^{\Delta 7,10,13,16}$, 22:5n3$^{\Delta 7,10,13,16,19}$, 22:5n6$^{\Delta 4,7,10,13,16}$, or 22:6n3$^{\Delta 4,7,10,13,16,19}$.

0006-3495/94/12/2387/07 $2.00

Raman spectroscopic studies (Litman et al., 1991). Information regarding less unsaturated species are available primarily for the 20:4n6 species but are sparse (i.e., 18:2n6, 18:3n3) or nonexistent (i.e., 22:5n6, 22:5n3) for other polyunsaturated species.

Previous differential scanning calorimetry (DSC) studies of mixed-chain polyunsaturated phospholipids have shown that the first two double bonds per *sn*-2 acyl chain lowers the gel to L_α transition temperature (Coolbear et al., 1983). Additional *sn*-2 unsaturation increased the transition temperature slightly, indicating that these lipids have a preference for the gel-state. In our study, a series of mixed-chain polyunsaturated phosphatidylcholine species that differ at the *sn*-2 position by chain length (18, 20, or 22 carbons), degree of unsaturation (1–6 double bonds), and location of the polyene segment (n-9, n-6, or n-3) was investigated. The study compares various long chain polyunsaturates with respect to thermodynamic properties of their gel to liquid-crystalline phase transition.

MATERIALS AND METHODS

Phospholipids

All phosphatidylcholines were obtained from either Matreya, Inc. (Pleasant Gap, PA) or Avanti Polar Lipids (Birmingham, AL) and contained 18:0 at the *sn*-1 glycerol position and one of the following unsaturated fatty acids at the *sn*-2 position: 18:1n9, 18:2n6, 18:3n6, 18:3n3, 20:2n6, 20:3n6, 20:4n6, 20:5n3, 22:4n6, 22:5n3, 22:5n6, or 22:6n3. Phospholipids were dissolved in chloroform containing butylated-hydroxytoluene (BHT) (1:250 BHT:lipid) and stored under nitrogen at −80°C. Phospholipid class purity was determined to be >99% by thin layer chromatography on a silica-coated plate using chloroform-methanol-water, 65:25:4. The stated acyl chain composition was found to be >98% as determined by fatty acid methyl ester analysis using a gas chromatograph equipped with a flame ionization detector (Knapp and Salem, 1989). The molecular weights of the phospholipid species were verified with liquid chromatography-mass spectrometry (Kim and Salem, 1987). These lipids were all found to contain <2% oxidized species as indicated by analysis with a modified HPLC method (Holte et al., 1990) using a reverse phase C18 column with 100% methanol and an ultraviolet detector set at 206 and 234 nm. The phospholipids, including the 22:6n3 species, contained <1% of the oxidized species as indicated by the second derivative of the 234 nm chromatograph. The synthetic 22:5n6 species required additional purification by reversed phase HPLC before phospholipid synthesis to remove *trans* isomers.

Differential scanning calorimetry

Samples were prepared by placing 1–10 mg of lipid in chloroform into an aluminum sample pan, drying under a stream of nitrogen and/or argon, and weighing on a microbalance under a N_2/Ar atmosphere to determine the amount of lipid present. An excess (5 μl) of deionized and degassed water was added, and the crucible was sealed under a nitrogen atmosphere. Measurements were made on a Mettler (Hightstown, NJ) DSC-30 differential scanning calorimeter equipped with a heating-cooling controller (range = −170–600°C). Melting points were determined in heating runs (scan range −40 to +20°C, scan rate 1–5°C/min). The values reported in Table 1 were derived from scans recorded at a rate of 3°C/min. For suitable samples, heating scans were also performed in the presence of supercooled water by scanning from −12 to 10°C. Cooling runs with supercooled water were scanned from 20 to −30°C. Cooling scans in the presence of ice were possible by precooling the samples to <−20°C and then increasing the temperature up to −2°C before beginning a −2 to −30°C run. The mean peak temperature of the transition and transition enthalpies were determined by integration of transition peaks. The peak baseline was set using the intercepts of the peak slope tangents with the baseline. The onset temperature of the transition was determined from the intercept of the baseline and the tangent of the slope of the transition curve. Multiple scans were made for each scan rate and direction. Three samples were analyzed for each species containing 18:1n9, 18:2n6, 20:2n6, 20:4n6, and 22:6n3; all other species samples were prepared twice. Scan rates of 1–10°/min were employed. Measured enthalpies increased with decreasing scan rate, but the sensor noise also increased. Peak temperatures and widths of transition were not different for the 1–3°/min scanning rates. We report the 3°/min data because of the low noise and reproducible enthalpies. A plot of enthalpy versus scan rate indicated 0°/min enthalpies between 6 and 12% greater than the 3°/min scanning runs, which is the same order of magnitude of the error associated with these measurements. Hence, the 3°/min data presented here accurately reflect the thermodynamics of the gel to liquid-crystalline phase transitions of our samples.

RESULTS

To illustrate the influence of increasing unsaturation upon the thermodynamics of the gel to liquid-crystalline transition for these mixed-chain polyunsaturated phosphatidylcholines, the results were grouped according to their *sn*-2 fatty acid chain length (18, 20, and 22 carbon families). Representative DSC scans of these mixed-chain polyunsaturated phosphatidylcholines are given in Fig. 1. Calorimetric data derived from the DSC scans are presented in Table 1. In Fig. 2, a plot of the peak transition temperature versus number of double

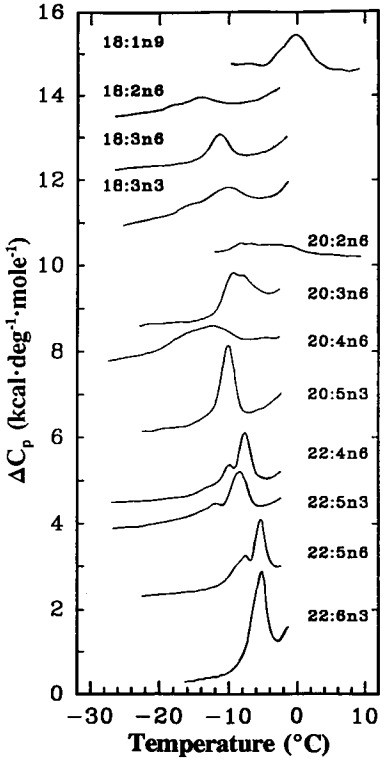

FIGURE 1 Normalized endotherms of representative heating scans of the mixed-chain unsaturated PCs containing 18:0 at the *sn*-1 position and the unsaturate indicated at the *sn*-2 position. Curves were shifted on the *y* axis for ease of presentation. Samples were scanned at 3°/min. All samples shown were in the presence of ice except for the 18:1n9 and 20:2n6 species, which were scanned in the presence of supercooled water.

TABLE 1 DSC of mixed-chain phosphatidylcholines

	Heating scan				Cooling scan			
sn-2 chain	*T* onset (°C)	*T* peak (°C)	ΔH (kcal/mole)	ΔS (cal/mol K)	*T* onset (°C)	*T* peak (°C)	ΔH (kcal/mole)	ΔS (cal/mol K)
18:1n9	−4.5 (0.2)	−0.1 (0.1)	4.9 (0.1)	17.8 (1.0)	3.1 (0.2)	−2.2 (0.2)	5.0 (0.4)	18.5 (1.3)
18:2n6	−21.4 (0.6)	−14.6 (0.1)	1.7 (0.1)	6.7 (0.2)	−11.1 (0.5)	−15.8 (0.1)	1.9 (0.2)	7.4 (0.5)
18:3n6	−14.0 (1.2)	−11.0 (0.7)	3.7 (0.4)	14.0 (1.4)	−9.5 (0.1)	−12.7 (0.9)	3.8 (0.3)	14.6 (1.0)
18:3n3	−18.8 (0.2)	−12.2 (0.3)	3.5 (0.6)	13.3 (2.3)	−8.5 (0.3)	−13.6 (0.3)	3.0 (0.2)	10.3 (0.5)
20:2n6	−12.0 (0.4)	−5.4 (0.3)	2.9 (0.3)	10.8 (1.1)	−4.4 (0.6)	−4.4 (0.6)	3.0 (0.1)	11.3 (0.2)
20:3n6	−14.0 (1.1)	−9.3 (0.7)	4.3 (0.4)	16.4 (1.4)	−7.8 (0.3)	−10.7 (0.8)	4.1 (0.5)	15.7 (1.9)
20:4n6	−18.6 (2.6)	−13.2 (0.8)	4.6 (0.6)	17.5 (2.5)	−10.3 (1.0)	−16.2 (1.0)	4.2 (0.3)	16.5 (1.2)
20:5n3	−13.1 (0.1)	−10.4 (0.1)	5.5 (0.1)	21.1 (0.4)	−10.5 (0.1)	−11.8 (0.1)	5.4 (0.1)	20.6 (0.3)
22:4n6	−13.8 (0.8)	−8.5 (0.1)	4.8 (0.2)	18.2 (0.9)	−8.1 (0.1)	−10.0 (0.1)	4.4 (0.1)	16.5 (0.1)
22:5n3	−16.6 (0.4)	−9.1 (0.4)	4.3 (0.1)	16.4 (0.4)	−8.6 (0.2)	−10.7 (0.3)	4.6 (0.1)	17.5 (0.3)
22:5n6	−12.3 (0.6)	−6.4 (0.2)	4.4 (0.6)	16.5 (2.2)	−6.2 (0.2)	−7.8 (0.3)	4.7 (0.4)	17.7 (1.4)
22:6n3	−8.7 (0.3)	−5.6 (0.3)	6.1 (0.4)	22.7 (2.4)	−5.7 (0.2)	−7.6 (0.3)	5.2 (0.2)	19.7 (0.7)

Data were acquired with a 3°C/min scan rate and represent the mean for an $n = 3$ for the 18:1n9, 18:2n6, 20:2n6, 20:4n6, and 22:6n3 species and an $n = 2$ for all others. All heating scan data in this table were measured in the presence of ice, with the exception of the 18:1n9 and 20:2n6 species (measured in supercooled water). Numbers in parentheses indicate the ± range of values for the given mean.

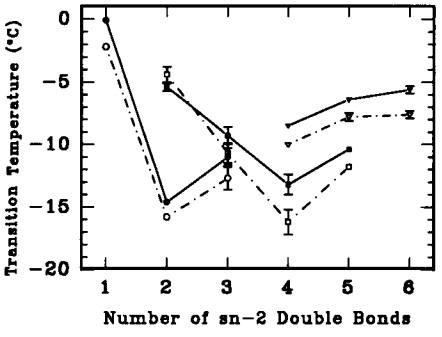

FIGURE 2 Peak melting temperatures (°C) of the gel to liquid-crystalline phase transitions as a function of *sn*-2 acyl chain length and degree of unsaturation. Solid lines are melting curves, and dotted lines are cooling curves. Circles, squares, and triangles represent the 18, 20, and 22 carbon chain length *sn*-2 acyl chains, respectively. The 18:3 species data are for 18:3n6, whose melting data were very similar to those of the 18:3n3 species; the 22:5 species was 22:5n6. Error bars represent the range for sample measurements. Some error bars are smaller than the symbols.

bonds at the *sn*-2 position for each of these groups is shown. For the 18 carbon family, we see that in going from one to two double bonds (18:1n9 to 18:2n6) the transition temperature has dropped more than 15°C, suggesting a loss of gel-state bilayer stability. The addition of a third double bond (18:3n3 or 18:3n6) resulted in an increase in the transition temperature. Addition of two or more *cis* double bonds to the 18 carbon length *sn*-2 chain does not result in a monotonic decrease in the main transition temperature. Both 18:3n6 and 18:3n3 increased the transition temperature equally in comparison with 18:2n6. These results are similar to those reported by Coolbear et al. (1983) for the 18:2n6 and 18:3n3 species. For the 18 carbon family, the lowest T_m is reached with 18:2n6. Subsequent addition of unsaturation beyond two double bonds increases T_m, independent of the position of the third double bond (i.e., n6 vs. n3). The heating and cooling scans resulted in peak T_m values that typically differed by 2°C for all species. All of the values in Table 1, except for the 18:1n9 species, are of transitions occurring in the presence of ice for both heating and cooling scans. In the case of 18:0,18:1n9-PC, the transition could only be observed when the water was in a supercooled state caused by the overlap with the melting of ice at 0°C. The effect of ice on the gel to liquid crystalline phase transition was observed for the 20:2n6 and 22:6n3 species because of the ability to resolve their transitions in both ice and supercooled water for both heating and cooling scans. The gel to liquid-crystalline transitions of these two species in the presence of supercooled water resulted in T_m (°C) and ΔH (cal/mol K) values that were ≤10% lower than that measured when ice was present. Therefore, the presence of supercooled or frozen water appeared to have little differential effect upon the measured phase transitions of the mixed-chain polyunsaturated phosphatidylcholines in this study.

For phospholipids containing 20 carbons at the *sn*-2 position, the increase in unsaturation from 20:2n6 to 20:3n6 to 20:4n6 resulted in a steady decrease in the transition temperature. However, upon the addition of a fifth double bond (20:5n3) the transition temperature increased. For the 22 carbon family, within the n6 and n3 species, a trend toward increasing transition temperature was observed with increasing unsaturation. The peak transition temperature increased in going from 22:4n6 (−8.5°) to 22:5n6 (−6.4°C) for the n6 lipids. T_m of the n3 species increased from −9.1°C for 22:5n3 to −5.6°C for the 22:6n3 species. We found that 18:0,22:6n3-PC resulted in the highest phase transition temperature (−5.6°C) of all the highly unsaturated species studied, i.e., those containing more than two double bonds. The onset temperatures of the transition reflect the same trends observed for the plot of peak transition temperature. We observed for each of the three groups (18, 20, or 22 carbon length at the *sn*-2 position) that there is a maximum level of unsaturation that results in the lowest T_m; further unsaturation results in an increase in the transition temperature. The unsaturated species resulting in the lowest transition temperature for each of the three families was 18:2n6 (18C), 20:4n6

(20C), and 22:5n3 (22C). Hernandez-Borrell and Keough (1993) reported multiple overlapping transitions in their study of mixed-chain polyunsaturated PCs containing 16:0 at the *sn*-1 position. We also observed varying degrees of multimodal transition behavior for these mixed-chain species containing 18:0 at the *sn*-1 position. These multiple overlapping transitions were most readily resolved in scans that were minimally overlapped by the ice transition. Neither we nor Keough's group can explain these multicomponent transitions based on analytical data of acyl chain composition or the presence of oxidized species, although extent of acyl chain migration was not determined. However, heterogeneous melting transitions are consistent with the microclustering of mixed-chain polyunsaturates reported by Litman et al. (1991). The NMR studies of Deese et al. (1981) and Barry et al. (1991) of 16:0,22:6n3-PC report an 8–10°C hysteresis between their heating and cooling runs. However, for 18:0,22:6n3-PC a 2.4°C hysteresis was measured (Barry et al., 1991). This is consistent with the 1–2°C hysteresis observed in our study. The DSC study of Hernandez-Borrell and Keough (1993) also reported no significant hysteresis for the 16:0 containing mixed-chain polyunsaturates. Some of the differences in results between DSC and spectroscopic studies may be caused by the rate of temperature ramping. Fast scan rates (3–5°C/min) are required in DSC studies, whereas temperature scans in spectroscopic studies are raised much more slowly.

Fig. 3 shows a plot of transition enthalpy versus number of double bonds for each of the three families (18, 20, or 22 carbon length at the *sn*-2 position). The two diene species (18:2n6 and 20:2n6) resulted in the lowest enthalpies (1.7 and 2.9 kcal/mole, respectively). This minimal enthalpy is consistent with a poorly packed gel-state bilayer organization. Coolbear et al. (1983) reported an enthalpy of 3.3 kcal/mole for 18:0,18:2n6-PC, which was the lowest of their series as well. Hernandez-Borrell and Keough (1993) observed

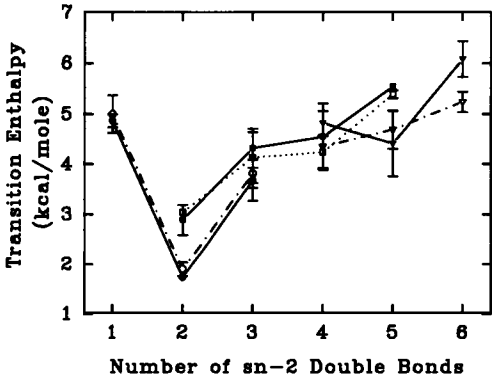

FIGURE 3 Transition enthalpy as a function of *sn*-2 acyl chain length and degree of unsaturation. Solid lines are melting curves, and dotted lines are cooling curves. Circles, squares, and triangles represent the 18, 20, and 22 carbon chain length *sn*-2 acyl chains, respectively. The 18:3 species data are for 18:3n6, whose melting data were very similar to those of the 18:3n3 species; the 22:5 species was 22:5n6. Error bars represent the range for sample measurements. Some error bars are smaller than the symbols.

a ΔH of 2.62 kcal/mole for 16:0,18:2n6-PC, the lowest for a polyunsaturated series containing 16:0 at the *sn*-1 position. Increasing the *sn*-2 acyl unsaturation from 18:2n6 to the 18:3n3 or 18:3n6 species resulted in a 1–2 kcal/mole increase in the transition enthalpy. Increasing unsaturation from 20:2n6 to the 20:3n6 species increased ΔH by 1 kcal/mole. Keough et al. (1987) also showed a minimization of ΔH with two double bonds (20:2n6) and an increase ($\approx$2 kcal/mole) with the 20:3 species in a series of mixed acid PCs with 20:0 at the *sn*-1 position in reasonable agreement with our results. Their study showed a decrease in ΔH with the 20:0,20:4n6 species, in contrast to our result with the *sn*-1 18:0,20:4n6 species. The low ΔH they measured for the 20:4n6 species may have been because of the transition being distorted by the ice peak interfering with peak analysis. All other species in their study had transitions that occurred above the melting point of ice. Some of our melting curves partially overlapped with the ice transition and made measuring ΔH difficult, particularly for 18:1n9 and 20:2n6. Heating and cooling scans in the presence of supercooled water allowed for analysis of these lipids. Also, subtraction of the ice peak from the 20:2n6 sample heating run gave ΔH values that were within 5% of the ΔH values derived from scans of the 20:2n6 species in supercooled water. The enthalpies we measured for the 20 carbon family species do not follow the same trend as seen for their transition temperatures. Beyond 20:2n6, T_m decreases while ΔH increases. However, the large fractional increase in ΔH (>20%) suggests an overall stabilization of the gel-state bilayer. A steady increase in ΔS as *sn*-2 unsaturation increases beyond 20:2n6 is clearly observed (Table 1).

For the 22 carbon series, only the 4, 5, and 6 double-bond members of this family were available for analysis. There was little difference in the transition entropies of the 22:4n6, 22:5n3, and 22:5n6 species. The 22:5n6 species had a higher T_m than the 22:4n6 and 22:5n3 species in both heating and cooling modes, but the transition enthalpies varied in a narrow range between these samples. The addition of a single double bond increased T_m and ΔH by 3.5°C and 1.8 kcal/mole, respectively, as can be observed by a comparison of the results obtained for 22:5n3 and 22:6n3. There was a similar difference between 22:5n6 and 22:6n3 species. It is clear that 18:0,22:6n3-PC resulted in the highest ΔH (6.1 kcal/mole) and highest T_m (−5.6°C) measured for any of our samples containing three or more double bonds.

DISCUSSION

Effect of one and two double bonds

Early investigations showed that the incorporation of a single double bond into the acyl chain of a phospholipid lowers its phase transition temperature (Ladbrooke and Chapman, 1969) and that the placement of this double bond near the center of the acyl chain resulted in maximal depression of the transition temperature (Barton and Gunstone, 1975). Furthermore, increasing the *sn*-2 unsaturation of a mixed-chain PC from 18:2n6 to 18:3n3 caused a 3–4°C increase in the

transition temperature (Coolbear et al., 1983) as was confirmed in the present study. Our results indicate that for the 18 carbon *sn*-2 chain length series, the presence of two *cis* double bonds (diene) in the *sn*-2 acyl chain of a mixed-chain phosphatidylcholine bilayer resulted in the lowest ΔH, ΔS, and T_m values, whereas increasing the unsaturation from two to three double bonds significantly increased ΔH, ΔS, and T_m. For the 20 carbon chain length series, enthalpy increased consistently with increasing unsaturation beyond two double bonds. These findings indicate that the gel-state at the gel to liquid-crystalline transition is maximally disrupted in mixed-chain PC bilayers containing diene *sn*-2 species (18:2n6 and 20:2n6) and increasing the unsaturation of these species stabilizes the gel-state bilayer structure.

Care must be taken when interpreting calorimetric data. It is assumed that the bilayer structure changes during the gel to liquid-crystalline phase transition from a single gel-state to a single liquid-crystalline state. We cannot exclude the possibility that a mixture of gel or liquid-crystalline phases may be present. Corresponding NMR, x-ray, or neutron diffraction data would be required to explore this question. Keough and co-workers interpreted their DSC results of the effects of increasing *sn*-2 unsaturation upon bilayer organization in a model that combines the interplay of a variety of inter- and intramolecular dynamics. Their formulation (Coolbear et al., 1983, Eq. 4) included approximations of partition functions for short-range repulsive interactions, long-range attractive forces, and chain conformation functions including area per molecule for both a saturated *sn*-1 chain and an unsaturated *sn*-2 chain. Other aspects such as chain tilt, leaflet interdigitation, and the effect of low temperature on the hydration shell may play a role in the resulting effects observed here, but cannot be addressed without further experimental evidence.

Low transition enthalpies observed for the 18 and 20 carbon dienes are consistent with the presence of a maximally perturbing *sn*-2 acyl chain conformation. Such a perturbed conformation is supported by recent NMR studies (Baenziger et al., 1992) of a mixed-chain deuterated 18:2n6 phosphatidylcholine. The authors conclude that it is likely that the 18:2n6 chain assumes a maximal tilt conformation where both double bonds of the diene unit are perpendicular to the bilayer normal. This conformation would be expected to be much more difficult to pack alongside saturated acyl chains than would a polyunsaturated chain in the hypothetical "angle iron" configuration (Applegate and Glomset, 1986). Addition of a third double bond may alter a tilted diene configuration by creating a rigid triene segment that may be less conformationally able to remain in a configuration tilted perpendicular to the bilayer normal. Increased transition enthalpies measured for the 18:3n6 and 18:3n3 species are consistent with a decreased occurrence of a perturbing conformation. The 18:2n6 and 20:2n6 species also show the smallest ΔS on melting, indicating a poorly ordered gel-state, consistent with the presence of a tilted diene conformation that does not pack well in the gel-state. We would predict the existence of such a structure for the mixed-chain phosphatidylcholines containing 16:2n6 or 22:2n6 at the *sn*-2 position as well.

Effect of three or more double bonds

Our data also show increasing ΔH and ΔS values as *sn*-2 unsaturation continues beyond three double bonds to the maximally nonconjugated *cis*-unsaturated state (i.e., 20:5n3 and 22:6n3, for the 20 and 22 carbon length chains, respectively). In the case of a mixed-chain (*sn*-1 saturate, *sn*-2 unsaturate) PC bilayer, it has been previously hypothesized (Coolbear et al., 1983; Litman et al., 1991) that bilayer stability can be explained as a function of interchain Van der Waals attractions that are dependent upon the degree of *sn*-2 unsaturation. When the *sn*-2 chain of a phospholipid achieves a maximal number of nonconjugated, *cis*-unsaturated double bonds (i.e., 20:5n3 and 22:6n3), the number of *sn*-2 *trans-gauche* conformations and available *sn*-2 hydrogens are minimal. This would be expected to result in fewer and/or weaker Van der Waals interactions between *sn*-1 and *sn*-2 acyl chains of the same phospholipid molecule. As a result, the saturated *sn*-1 chains may have preferential Van der Waals attractions with saturated *sn*-1 chains on neighboring molecules. Enthalpies of PCs containing two polyenoic chains (e.g., di20:4n6-PC) are on the order of 1–2 kcal/mole (Keough and Kariel, 1987), whereas we observed for 18:0,20:4n6-PC a ΔH of 4.6 kcal/mole, supporting the idea that the saturated *sn*-1 acyl chains of mixed-chain PCs in our study contribute to the increased bilayer order of the gel-state. Increased occurrence of stronger interactions between neighboring *sn*-1-saturated chains would predictably increase ΔH. One could speculate that such longer-range interactions would occur transiently and possibly have a lifetime that increases with the degree of *sn*-2 unsaturation. Such a preferred conformation could result in the formation of transient microclusters or lattices in the plane of the bilayer. Evidence for such interactions were suggested from a Raman spectroscopy study of 1–16:0,2–22:6n3-PC by Litman et al. (1991). The authors proposed that 22:6n3-containing PC microclusters resulted from long-lived Van der Waals interactions between neighboring *sn*-1 acyl chains. Our data are consistent with these observations. Increasing unsaturation significantly increases ΔS in the 20 and 22 carbon families, particularly when going to the maximally unsaturated state of each family (20:4n6 → 20:5n3 and 22:5n3 → 22:6n3). Other maximally unsaturated lipids (i.e., 16:3n3 and 18:4n3) would also be predicted to exhibit this ordering behavior. The relatively narrow and high enthalpic gel to liquid-crystalline phase transition of the 22:6n3 species may represent a preferential melting of these stronger *sn*-1/*sn*-1 chain interactions. The interactions between the *sn*-1 18:0 chains and the *sn*-2 22:6n3 acyl chains may only weakly contribute to the total transition enthalpy.

Comparison of n6 vs. n3 polyunsaturates

By comparing phospholipids that contain 18:3n3 vs. 18:3n6 and 22:5n3 vs. 22:5n6 at the *sn*-2 position, the importance of

double-bond placement (n3 vs. n6) for species having the same chain length and number of double bonds can be discerned. Similar T_m, ΔH, and ΔS values suggest that the stabilization of the bilayer caused by increasing polyunsaturation was not dependent upon the location (Δ6, 9, 12 vs. Δ9, 12, 15 for 18:3n6 and n3, and Δ7, 10, 13, 16, 19 vs. Δ4, 7, 10, 13, 16 for 22:5n3 and n6) of the double bonds. However, a more heterogeneous membrane containing cholesterol, proteins, or other components may be more suitable than one-component PC bilayers for investigating the differential structural role of n3 vs. n6 lipids. These DSC results agree with steady-state fluorescence polarization measurements (Ehringer et al., 1991) showing no difference between mixed acid PCs containing either 18:3n3 or 18:3n6. It is very clear, however, that 22:5n3 and 22:5n6-containing phospholipid bilayers exhibit significantly less enthalpy change (4.3 and 4.4 kcal/mole, respectively) during the gel to liquid-crystalline transition than those containing 22:6n3 (6.1 kcal/mole). In these pure mixed-chain PC systems, ΔH of the gel to liquid-crystalline phase transition of bilayers containing long-chain (20–22 carbons) unsaturated fatty acids with more than four double bonds are more dependent upon the degree of *sn*-2 polyunsaturation than on the chain position (n3 vs. n6) of the double bonds. Mixed-chain phospholipids with a saturated *sn*-1 chain and a polyunsaturate at the *sn*-2 position provide a more diverse range of acyl chain interactions and conformations that are not available in the less common diunsaturated species (containing two polyenoic chains).

Special properties of docosahexaenoic acid, 22:6n3

Mixed-chain PC species containing 22:6n3 have the highest ΔH and ΔS when compared with other polyunsaturated species, suggesting a well ordered gel-state bilayer structure. Loss of just one double bond (22:5n6 and 22:5n3) decreases these maximal transition enthalpy and entropy values. These data are the first reported physical differences between bilayers containing 22:6n3 versus those containing 22:5n6. It is surprising that a difference of one double bond between 22:5n6 and 22:6n3 can result in a significant difference in the transition enthalpy of bilayers containing these mixed-chain PC species. Such a physical difference between these two phospholipid species may contribute, in part, to the neuropathology associated with omega-3 fatty acid deficiency and chronic alcoholism where a lower 22:6n3/22:5n6 ratio is observed (Salem and Pawlosky, 1994; Salem and Ward, 1993).

In light of past structural studies, our DSC results suggest that the maximally unsaturated 22:6n3 species are capable of a unique combination of conformational and structural interactions. The large cross sectional area of the 22:6n3-containing phospholipid results in faster fluorescent probe correlation times, shorter fluorescence lifetimes, and more degrees of probe freedom, all of which are consistent with a disordered acyl chain environment (Straume and Litman, 1987; Salem and Niebylski, 1993; Stubbs, 1993; Niebylski and Salem, 1994). Yet the large ΔH and ΔS observed for the 22:6n3 species suggests that this phospholipid has a very ordered and well packed gel-state conformation. It is possible that some of the unique gel-state packing properties occur transiently in the L_α state. Increasing the degree of *sn*-2 unsaturation appears to result in stronger acyl chain packing in the gel-state of mixed-chain PC bilayers. However, in the liquid-crystalline state, fluorescence data suggest that increasing *sn*-2 unsaturation results in greater degrees of probe freedom and an increased fractional packing volume, indicating a decrease in bilayer order. Comparison of other highly unsaturated species does not demonstrate the same large relative difference between gel-state ordering and L_α disordering that is observed for the 22:6n3-containing species. For example, as compared with 22:6n3 species, mixed-chain PC containing 20:4n6 has a more ordered acyl chain environment as interpreted from longer (slower) fluorescence probe correlation times (Straume and Litman, 1987; Salem and Niebylski, 1993; Niebylski and Salem, 1994). However, the 18:0,20:4n6 species has a significantly lower ΔH compared with the 18:0,22:6n3 species. These data indicate that 18:0,20:4n6-PC has a less well ordered gel-state and a more ordered L_α state than 18:0,22:6n3-PC. Furthermore, this trend holds true for all other mixed-chain unsaturated PC species containing 18:0 that we have analyzed with both methods (Niebylski and Salem 1994; our unpublished observations). However, Hernandez-Borrell and Keough (1993) have reported that 16:0,22:6n3-PC has a smaller ΔH (4.11 kcal/mole) than does 16:0,20:4n6-PC (5.40 kcal/mole). This indicates that the *sn*-1 saturate chain is important for the gel-state ordering of the mixed-chain polyunsaturates. A longer *sn*-1 saturated chain will better promote the gel-state order of the long chain polyunsaturates. This may be of particular significance because there is an increased prevalence of 18:0 containing mixed-chain polyunsaturated phospholipids in the brain, retina, and sperm (Salem et al., 1976, 1986).

The particular conformation and interactions imparted by 22:6n3-containing mixed-chain phospholipids may contribute to optimal membrane-bound protein function, as has been described for rhodopsin (Mitchell et al., 1992). Protein conformational changes during activation and bulky peptide side chains may require a high degree of free volume in the fatty acyl chain region near the lipid-protein interface. At the same time, the biological membrane must also maintain optimal structural integrity, particularly at the synapse where an impermeable membrane can help preserve maximal transmembrane ion gradients. The presence of mixed-chain 22:6n3-containing phospholipids in a membrane would promote both of these diverse structural requirements. Such a unique capability may explain why synaptosomal and rod outer segment membrane phospholipid is enriched in 22:6n3 and why the nervous system is highly resistant to its depletion (Salem et al., 1986, 1989). The unique bilayer organizational properties of 22:6n3 may underlie its essential role in the nervous system.

The authors would like to thank Dr. Klaus Gawrisch and Dr. Burton Litman for their many helpful discussions.

C. D. Niebylski completed this work while supported by a National Research Council Associateship. Portions of this work have been published in abstract form in *Biophysical Journal* 66:56*a*. (Abstr.).

REFERENCES

Applegate, K. R., and J. A. Glomset. 1986. Computer-based modeling of the conformation and packing properties of docosahexaenoic acid. *J. Lipid Res.* 27:658–680.

Barry, J. A., T. P. Trouard, A. Salmon, and M. F. Brown. 1991. Low temperature ^2H NMR spectroscopy of phospholipid bilayers containing docosahexaenoyl (22:6ω3) chains. *Biochemistry.* 30:8386–8394.

Baenziger, J. E., H. C. Jarrell, and I. C. P. Smith. 1992. Molecular motions and dynamics of a diunsaturated acyl chain in a lipid bilayer: implications for the role of polyunsaturation in biological membranes. *Biochemistry.* 31:3377–3385.

Barton, P. G., and F. D. Gunstone. 1975. Hydrocarbon chain packing and molecular motion in phospholipid bilayers formed from unsaturated lecithins. Synthesis and properties of sixteen positional isomers of 1,2-dioctadeenoyl-sn-glycero-3-phosphorylcholine. *J. Biol. Chem.* 250: 4470–4476.

Coolbear, K. P., C. B. Berde, and K. M. W. Keough. 1983. Gel to liquid-crystalline phase transitions of aqueous dispersions of polyunsaturated mixed-acid phosphatidylcholines. *Biochemistry.* 22:1466–1473.

Deese, A. J., E. A. Dratz, F. W. Dahlquist, and M. R. Paddy. 1981. Interactions of rhodopsin with two unsaturated phosphatidylcholines: a deuterium NMR study. *Biochemistry.* 20:6420–6427.

Dratz, E. A., and A. J. Deese. 1986. The role of docosahexaenoic acid (22:6ω3) in biological membranes: examples from photoreceptors and model membrane bilayers. *In* Health effects of polyunsaturated fatty acids in seafoods. A. P. Simopoulos, R. R. Kifer, and R. Martin, editors. Academic Press, New York. 319–351.

Ehringer, W. D., D. Belcher, S. R. Wassall, and W. Stillwell. 1991. A comparison of α-linolenic acid (18:3ω3) and γ-linolenic acid (18:3ω6) in phosphatidylcholine bilayers. *Chem. Phys. Lipids.* 57:87–96.

Ghosh, D., M. A. Williams, and J. Tinoco. 1973. The influence of lecithin structure on their monolayer behavior and interactions with cholesterol. *Biochim. Biophys. Acta.* 291:351–362.

Hernandez-Borrell, J., and K. M. W. Keough 1993. Heteroacid phosphatidylcholines with different amounts of unsaturation respond differently to cholesterol. *Biochim. Biophys. Acta.* 1153:277–282.

Holte, L. L., F. J. G. M. Van Kuijk, and E. A. Dratz. 1990. Preparative high-performance liquid chromatography purification of polyunsaturated phospholipids and characterization using ultraviolet derivative spectroscopy. *Anal. Biochem.* 188:136–141.

Keough, K. M. W., B. Giffin, and N. Kariel. 1987. The influence of unsaturation on the phase transition temperatures of a series of heteroacid phosphatidylcholines containing twenty-carbon chains. *Biochim. Biophys. Acta.* 902:1–10.

Keough, K. M. W., and N. Kariel. 1987. Differential scanning calorimetric studies of aqueous dispersions of phosphatidylcholines containing two polyenoic chains. *Biochim. Biophys. Acta.* 902:11–18.

Kim, H.-Y., and N. Salem, Jr. 1987. Application of thermospray high-performance liquid chromatography/mass spectrometry for the determination of phospholipids and related compounds. *Anal. Chem.* 59: 722–726.

Kim, H.-Y., S. Sawazaki, and N. Salem, Jr. 1991. Lipoxygenation in rat brain? *Biochem. Biophys. Res. Commun.* 174:729–734.

Knapp, H. R., and N. Salem, Jr. 1989. Formation of PGI3 in the rat during fish oil supplementation. *Prostaglandins.* 38:509–521.

Ladbrooke, B. D., and D. Chapman. 1969. Thermal analysis of lipids, proteins and biological membranes. A review and summary of some recent studies. *Chem. Phys. Lipids.* 3:304–367.

Litman, B. J., E. N. Lewis, and I. W. Levin. 1991. Packing characteristics of highly unsaturated bilayer lipids: Raman spectroscopic studies of multilamellar phosphatidylcholine dispersions. *Biochemistry.* 30:313–319.

Mitchell, D. C., M. Straume, and B. J. Litman. 1992. Role of sn-1 saturated, sn-2 polyunsaturated phospholipids in control of membrane receptor conformational equilibrium: effects of cholesterol and acyl chain unsaturation on the metarhodopsin I $\leftrightarrow$ metarhodopsin II equilibrium. *Biochemistry.* 31:662–670.

Niebylski, C. D., and N. Salem, Jr. 1994. Time-resolved fluorescence anisotropy and differential scanning calorimetry of a series of mixed-acid phosphatidylcholine bilayers: effect of sn-2 acyl chain length and degree of unsaturation. *Biophys. J.* 66:56*a*. (Abstr.)

Salem, N., Jr. 1989. Omega-3 fatty acids: molecular and biochemical aspects. *In* New Protective Roles for Selected Nutrients. G. Spiller and J. Scala, editors. Alan R. Liss, Inc., New York. 109–228.

Salem, N., Jr., L. G. Abood, and W. Hoss. 1976. Separation of brain phosphatidylserines according to degree of unsaturation by thin-layer chromatography. *Anal. Biochem.* 76:407–415.

Salem, N., Jr., H.-Y. Kim, and J. A. Yergey. 1986. Docosahexaenoic acid: membrane function and metabolism. *In* Health Effects of Polyunsaturated Fatty Acids in Seafoods. A. P. Simopoulos, R. R. Kifer, and R. Martin, editors. Academic Press, New York. 263–317.

Salem, N., Jr., and C. D. Niebylski. 1993. An evaluation of alternative hypotheses involved in the biological functions of docosahexaenoic acid in the nervous system. *In* Essential Fatty Acids and Eicosanoids. A. Sinclair and R. Gibson, editors. American Oil Chemistry Society, Champaign, IL. 84–86.

Salem, N., Jr., and C. D. Niebylski. 1995. The nervous system has an absolute molecular species requirement for proper function. *Mol. Membr. Biol.* In press.

Salem, N., Jr., and R. J. Pawlosky. 1994. Health policy aspects of lipid nutrition and early development. *World Rev. Nutr. Diet.* In press.

Salem, N., Jr., and G. R. Ward. 1993. Are omega-3 fatty acids essential nutrients for mammals? *World Rev. Nutr. Diet.* 72:128–147.

Slater, S. J., M. B. Kelly, F. J. Taddeo, C. Ho, E. Rubin, and C. D. Stubbs. 1994. The modulation of protein kinase C activity by membrane lipid bilayer structure. *J. Biol. Chem.* 269:4866–4871.

Straume, M., and B. J. Litman. 1987. Equilibrium and dynamic structure of large, unilamellar, unsaturated acyl chain phosphatidylcholine vesicles. Higher order analysis of 1,6-diphenyl-1,3,5-hexatriene and 1-[4-(trimethylammonio)phenyl]-6-phenyl-1,3,5-hexatriene anisotropy decay. *Biochemistry.* 26:5113–5120.

Stubbs, C. D. 1993. The structure and function of docosahexaenoic acid in membranes. *In* Essential Fatty Acids and Eicosanoids. A. Sinclair and R. Gibson, editors. American Oil Chemistry Society, Champaign, IL. 116–121.

Stubbs, C. D., and A. D. Smith. 1984. The modification of mammalian membrane polyunsaturated fatty acid composition in relation to membrane fluidity and function. *Biochim. Biophys. Acta.* 779:89–137.

Wiedmann, T. S., R. D. Pates, J. M. Beach, A. Salmon, and M. F. Brown. 1988. Lipid-protein interactions mediate the photochemical function of rhodopsin. *Biochemistry.* 27:6469–6474.